CONF-9104171--5

F111 CREW ESCAPE MODULE PILOT PARACHUTE*

SAND--90-2124C

DE91 007573

Eden L. Tadios†

Sandia National Laboratories‡
Albuquerque, New Mexico 87185

ABSTRACT

The pilot parachute system which extracts the F111 Crew Escape Module recovery parachute system must provide reasonable bag strip velocities throughout the flight envelope (10 psf to 300 psf). The pilot parachute system must, therefore, have sufficient drag area at the lower dynamic pressures and a reduced drag area at the high end of the flight envelope. The final design that was developed was a dual parachute system which consists of a 5-ft diameter guide surface parachute tethered inside a 10-ft diameter flat circular parachute. The high drag area is sustained at the low dynamic pressures by keeping both parachutes intact. The drag area is reduced at the higher extreme by allowing the 10-ft parachute attachment to fail. The discussions to follow describe in detail how the system was developed.

INTRODUCTION

A successful deployment of a parachute system highly depends on the efficiency of the deployment device and/or method. There are several existing methods and devices that may be considered for a deployment system. For the F111 Crew Escape Module (CEM), the recovery parachute system deployment is inititated by the firing of a catapult that ejects the complete system from the CEM. At first motion of the pack, a drogue gun is fired, which deploys the pilot parachute system. The pilot parachute system then deploys the main parachute system, which consists of a cluster of three 49-ft diameter parachutes. The design specifications of the CEM recovery parachute system required successful operation of the parachute system at dynamic pressures (Q) ranging from 10 psf to 300 psf.

The unconventional deployment of the F111 CEM parachute system posed a challenge for the design and development of the complete system [1]. Because of the existing configuration of the compartment for the recovery system in the CEM, the system is deployed at an angle of attack under most conditions. The compartment is at 60 degrees with respect to the longitudinal axis on the CEM (Figure 1). Combined with high speed deployment and the compartment orientation, the parachute system is vulnerable to the linesail phenomenon and the results can be catastrophic. Under these conditions, deployment forces must be high enough to minimize linesail, but still maintain reasonable bag strip velocities. However, the same pilot parachute system must provide enough drag area at low speeds to provide sufficient bag strip velocities to rapidly deploy the main system. The requirements at the two extremes of the flight envelope necessitated the use of a variable drag area deployment device. Hereafter, drag area will be simply referred to as drag.

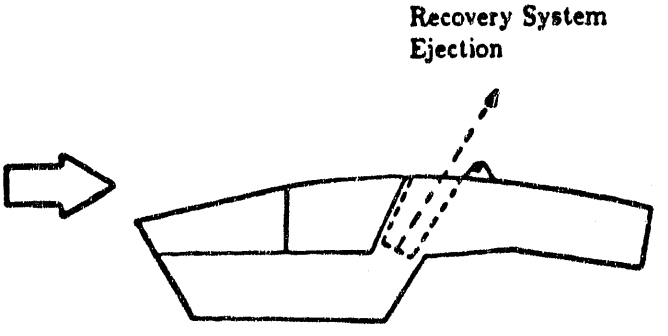

Figure 1: Crew Escape Module at Zero Angle of Attack

The variable drag problem was resolved with a dual parachute system. This system maintained the high drag when both parachutes remained intact. The low drag was achieved when the larger parachute's attachments failed. This released the larger parachute and drag was produced only by the smaller parachute. Wind tunnel drag data of the system and the individual parachutes are presented in Table 1.

Table 1: Wind Tunnel Drag Data

Configuration	C_DS ft^2	Wind Tunnel Q (psf)
5-ft Diameter	12.8	20
10-ft Diameter	58.0	2
5-ft/10-ft	52.0	5

*This work performed at Sandia National Laboratories supported by the U.S Air Force on Project Order SM-MMK-87-10-324

†Member Technical Staff, Member AIAA

‡This work performed at Sandia National Laboratories supported by the U.S. Department of Energy under contract number DE-AC04-76DP00789.

PARACHUTE SYSTEM DESCRIPTION

The final pilot parachute system design consists of a 5-ft diameter guide surface parachute tethered inside a 10-ft diameter flat circular parachute. The 10-ft diameter flat-circular parachute (outer parachute) canopy has 12 gores with 5/16" x 800-lb Kevlar suspension lines. The canopy is Nylon cloth, MIL-C-7020, 1.1 oz per square yard. The 5-ft diameter guide surface parachute (inner parachute) has a 12-gore canopy with 1" x 2400-lb Kevlar suspension lines. The canopy is made of MIL-C-7350, 2.25 oz per square yard Nylon cloth.

Drag was reduced by the failure of the 10-ft diameter parachute attachment at an approximate load of 2500 lbs (≈ 21 G's). The point of failure was at the loop joints (sewn onto the bridle) to which the suspension lines were attached (Figure 2). Failure occurred when the stitch pattern on the loop joints yielded to the suspension line loads.

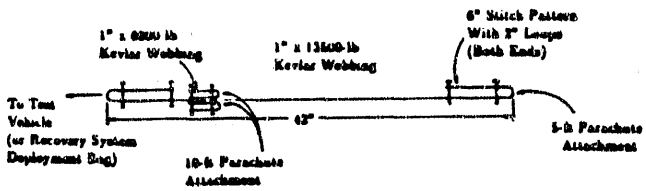

Figure 2: Loop Joint Bridle

Loop Joint Description

The loop joint system is constructed of a 1" x 13500-lb Kevlar bridle with 2-inch loops at each end having a 6-inch stitch pattern. The loop joints are sewn to the bridle with FF Nylon thread with a 2-inch long, 3-point stitch pattern with 9 stitches per inch. The desired failure load can also be obtained with Kevlar thread with a different pattern length, but Nylon thread provides a more consistent failure. A summary of the stitch patterns tested is included in Table 2. The geometry of the two parachutes determined the loop joint location and the bridle length.

Since the three-point stitch pattern has been known to fail in a more consistent manner compared to other patterns, it was chosen for this application. Loop joints with different stitch pattern lengths and threads were first tested at steady-state on a tensile test machine. If the average failure load was within 2500 ± 50 lbs, the selected pattern was then implemented in the system and consequently subjected to a deployment test. However, the process became a trial and error approach because failure loads from the deployment tests did not agree with previous tensile tests results.

The discrepancy between the steady-state and deployment tests results may be explained by the mechanics and geometry of a steady-state test versus a dynamic deployment test. The conventional steady-state test subjected the stitch pattern to shear stress only (Figure 3a). In a deployment test, both shear and tensile loads were applied on the stitch pattern (Figure 3b). Further investigation revealed that the stitch pattern was as much as an order of magnitude weaker in tension than in shear. In a deployment test, the loop joints failed largely due to tension, resulting in a much lower failure load. By inserting a diamond block within the test specimen, the dynamic load vector was modeled in the steady-state tests (Figure 4). This setup provided more reliable results as verified by the deployment tests.

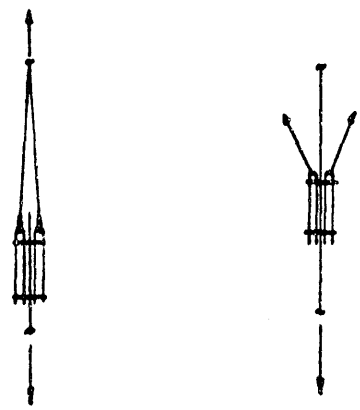

Figure 3: Steady-state (a) and Deployment (b) Tests Load Vectors

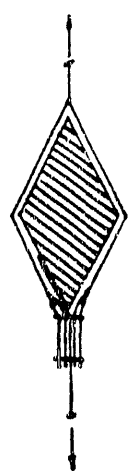

Figure 4: Modified Steady-state Test

TEST DESCRIPTION

The design was tested in two phases to verify that the requirements were met. The first phase was low Q tests and the second was high Q tests. A different test method was employed for each of the test phases, but the sequence of events were the similar. The terms low and high Q will be used interchangeably with low and high speeds, respectively, to refer to the deployment conditions.

Test Objectives and Methods

The primary objective of the low Q tests was to determine the transition point at which the stitchings failed, releasing the 10-ft parachute. For the low Q tests, the test unit was released from a helicopter at a predetermined release condition, which was obtained from the point mass trajectory simulation code, PBODY [2]. Simultaneously at release, a pin was pulled from the test unit, activating the time delay programmed into the onboard instrumentation. A pyrotechnic cutter was then electrically fired when the time delay expired, initiating the parachute system deployment sequence: a compressed spring was ejected, deploying a 2-ft guide surface parachute which extracted the pilot parachute system (Figure 5). This canopy-first deployment simulated the deployment from the main parachute for the CEM.

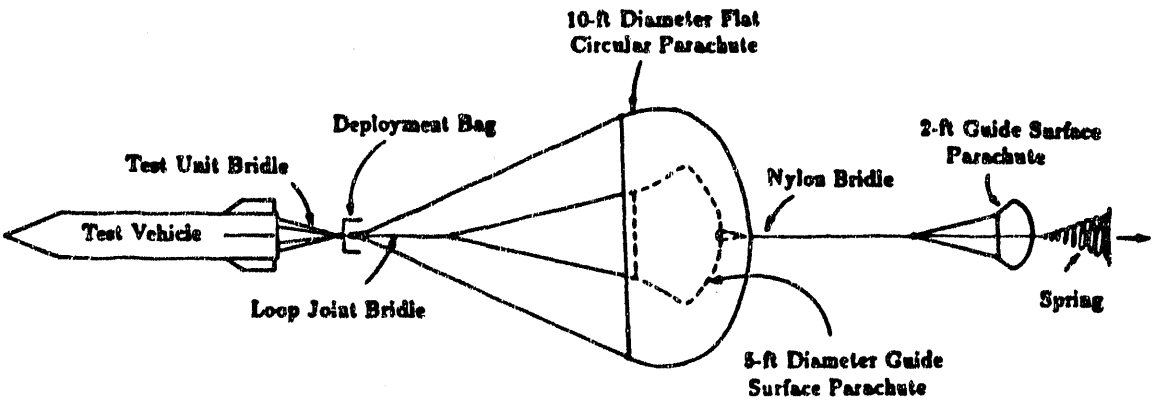

Figure 5: Deployment Sequence

The purpose of the high Q tests was to verify the structural integrity of the pilot parachute system. This required launching the test unit with an HVAR rocket to achieve the higher dynamic pressures of the flight envelope. After rocket burnout, drag plates attached to the rocket (Figure 7) forced separation from the test vehicle. The sequence of events after separation (free-flight) was similar to that in the drop tests, except the pin was pulled prior to rocket ignition. Parachute deployment was determined from combined trajectory simulations of the rocket stage and vehicle free-flight. The simulations were obtained from the six-degree-of-freedom code, AMEER [3]. In addition to the main parachute high Q tests data, one test provided the confidence in the system's structural integrity at high speed deployments.

Test Equipment

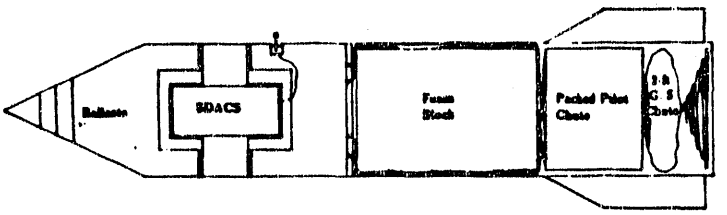

Figure 6: Test Unit Configuration

The pilot parachute sytem was deployed from a 9-inch diameter parachute test vehicle (Figure 6). The complete test unit weighed about 118 lbs, with the exception of the last two tests (22 psf and 41 psf) in which the unit weighed 116 lbs. The total weight of the test unit simulated the weight of the main parachute pack. Simulated trajectories showed that the two-pound difference did not have significant effects on the results. The onboard instrumentation, depicted in Figure 6, was the Stored Data Acquisition System (SDACS) [4] which recorded deceleration and activated the deployment mechanism. Three accelerometers within the SDACS unit measured the three components of deceleration in G's.

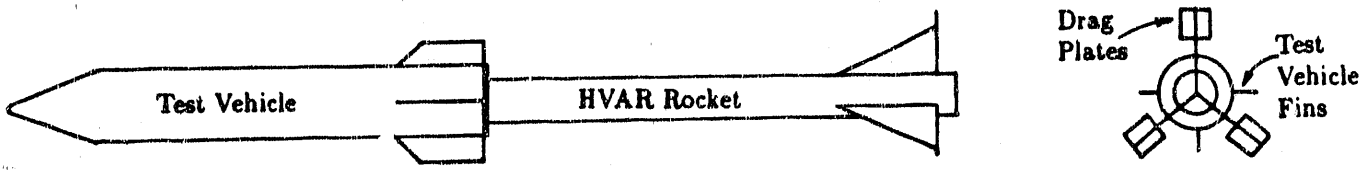

Figure 7: Rocket Test Setup Sideview and Endview

DATA ACQUISITION AND REDUCTION

The SDACS was the primary source of raw data. The maximum loads were computed from the SDACS data by multiplying the deceleration magnitude by the test unit weight. Trajectory data were also provided by a laser tracker, but reduction of the data to obtain the loads (dynamic pressure multiplied by the steady state drag area) was not as accurate as the SDACS because of the uncertainties in the effective drag area and inaccuracies in computing the dynamic pressure. The laser tracker data reduction had the added error associated with differentiation while the SDACS data did not. In addition to numerical data, photometric coverage was also provided for visual evaluations.

TEST RESULTS

A summary of the flight test program results is shown in Table 2. With respect to the dynamic pressure, the loads appear inconsistent in some cases. There are several possible reasons for the discrepancies. One explanation may be attributed to the uncertainties associated with dynamic pressure calculations. Winds could not be measured throughout any of the trajectories so the velocity profile was with respect to still air. The absence of winds in the dynamic pressure computations becomes additional error, since Q is a function of velocity squared. Typical deployment altitudes were between 1200 to 1500 AGL and winds were common at the test area at these altitudes.

One must also consider the inherent variables in a canopy-first deployment. These ultimately affect the stitchings and the loads. Consider the likelihood of a non-uniform canopy inflation. This produces an asymmetric loading on the suspension lines and on the two loop joints' stitchings. Additionally, the variability in the sewn loop joints cannot be overlooked as a source of what appear to be anomalies in the data.

The measured loads at the 20 psf and 22 psf tests for the final loop joint design are not consistent, perhaps because of reasons explained earlier. It is conceivable that, even with a 400 Hz sampling rate, a peak deceleration other than what was recorded may have been missed. With that premise, it is entirely possible that the peak load for the 22 psf test may be higher than 1181 lbs.

Typical SDACS data plots are shown in Figures 8 and 9. Figure 8 shows the load history when the outer parachute remains intact while Figure 9 presents the load history when the outer parachute fails. In Figure 8, the first peak is at line stretch and the second peak is at full canopy inflation of the outer parachute. The magnitude of the second peak was taken as the maximum load listed in Table 2.

Table 2: Test Program Data Summary

Stitch Pattern	Computed Q (psf)	Max Load (lbs)	Joint Failure
2", 3-pt,	18	806	No
9 spi, E Kevlar	39	1789	Yes
	43	2406	Yes
	57	1967	Yes
	79	2133	Yes
2 3/4", 3-pt,	33	1778	Yes
9 spi, E Kevlar	35	2275	Yes
	51	2358	Yes
2", 3-pt,	20	1825	No
9 spi, FF Nylon	22	1181	No
	39	3145	Yes
	41	3305	Yes
	242	4681	Yes

The first two peaks in Figure 9 have the same interpretation as in the previous figure. The third peak indicates full inflation of the inner parachute. Although the 10-ft diameter parachute was "released", it was still attached to the system at the vent. The parachute was then allowed to flutter behind the 5-ft diameter parachute. The flag drag could have contributed to the drag fluctuation that occurs after the third peak.

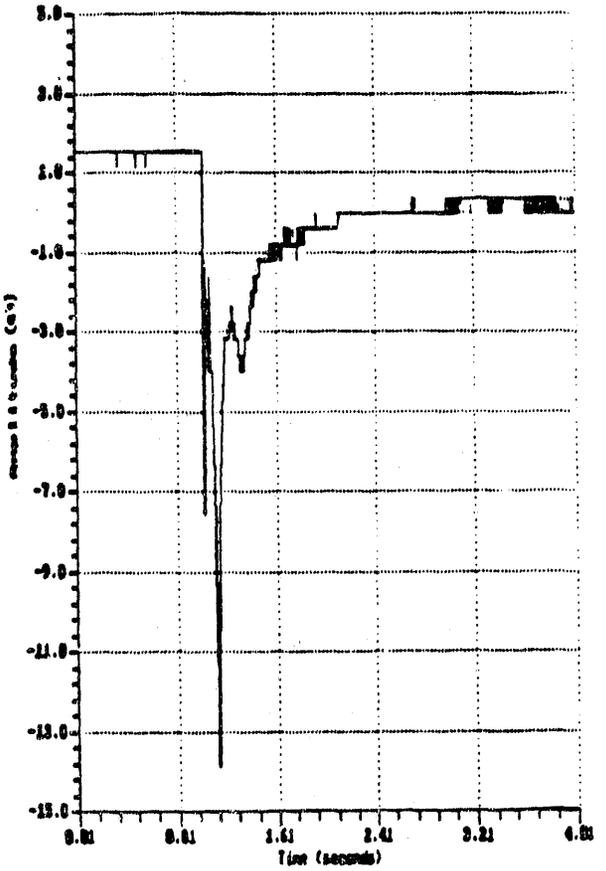

Figure 8: Load History: Outer Parachute Intact

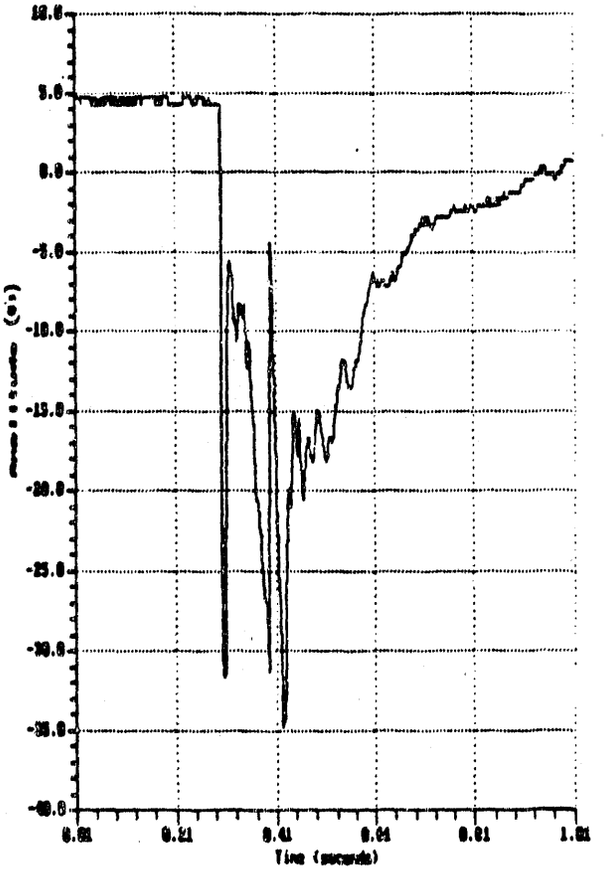

Figure 9: Load History: Outer Parachute Failure

Test data for the final design provide evidence that the main objective of the low Q tests has been satisfied. Figure 10 indicates that the desired 2500 lb failure load will occur at a dynamic pressure between 20 psf and 40 psf. The actual Q at which the loop joints fail will vary between these two conditions due to the capricious nature of canopy-first deployment. However, a linear approximation of the data indicates that failure will occur at about 32 psf.

CONCLUSIONS

Developing a variable drag device was not an easy task, but the efforts proved to be worthwhile with the dual parachute system. At low Q, the dual parachute geometry provides the necessary high drag profile to deploy the main system rapidly. At the other extreme, the outer parachute is released, leaving only the guide surface parachute to exert the drag. With a lower drag at high speeds, bag strip velocities are kept to reasonable levels, minimizing linesail. As the data can attest, the dual pilot parachute system has proven to be a viable variable drag device to deploy the F111 CEM recovery parachute system.

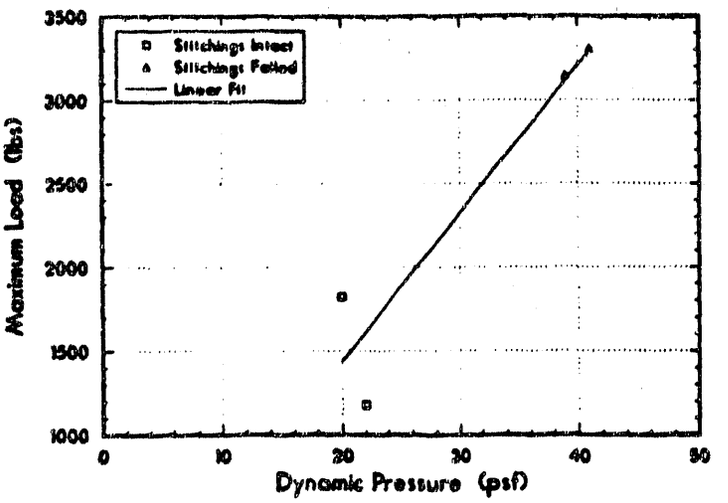

Figure 10: Loop Joint Transition Point

Acknowledgements

The author wishes to thank Don Johnson of Sandia National Labs (SNL) for his guidance throughout the development of this project and for providing helpful discussions and suggestions in producing this document. Thanks are also due to Don Waye (SNL) for his helpful sugggestions. The author also wishes to acknowledge Dan Luna, Larry Whinery, Gene Hauser (all of SNL) and the Sandia Labs Coyote Test Field Facilities for providing support throughout the program and to Terry Jordan (SNL) for providing technical assistance for the high Q tests.

References

[1] Johnson, D. W.; "Testing of a New Recovery Parachute System for the F111 Aircraft Crew Escape Module: An Update," AIAA 10th Aerodynamic Decelerator Systems Technology Conference; Cocoa Beach, Florida, Paper No. 89-0891-CP, April 1989.

[2] Purvis, J. W.; "Numerical Simulation of Decelerator Deployment," University of Minnesota Decelerator Systems Engineering Short Course, Albuquerque, New Mexico, July 1985.

[3] Meyer, Eugene J.; "A User's Manual for the AMEER Flight Path-Trajectory Simulation Code," Sandia Report No. SAND80-2056, December 1984.

[4] Ryerson, D. E. and Hauser, G. C.; "Small Parachute Flight Data Acquisition System," AIAA 10th Aerodynamic Decelerator Systems Technology Conference; Cocoa Beach, Florida, Paper No. 89-0924-CP, April 1989.

END

DATE FILMED

03/27/91